Received: 3 January 2019 | Revised: 26 April 2019 | Accepted: 13 May 2019

DOI: 10.1002/mmce.21861

RESEARCH ARTICLE

INTERNATIONAL JOURNAL OF RF AND MICROWAVE COMPUTER-AIDED ENGINEERING WILEY

# A double line SIW cavity backed antenna for WLAN applications

**Swaminathan Anand** | **D. Rokhini**

Department of Electronics and Communication Engineering, Mepco Schlenk Engineering College, Virudhunagar, Tamil Nadu, India

**Correspondence**
Swaminathan Anand, Department of Electronics and Communication Engineering, Mepco Schlenk Engineering College, Sivakasi 626005, Virudhunagar, Tamil Nadu, India.
Email: sanand@mepcoeng.ac.in

**Abstract**

A compact double line substrate integrated waveguide (DLSIW) cavity backed antenna is realized using half mode SIW technology for WLAN applications. The existing single line SIW antennas for WLAN applications have low gain and less efficiency. To overcome this limitation, DLSIW structure is proposed. The new DLSIW structure simultaneously achieves better gain, radiation efficiency, and good front to back ratio (FTBR) with compact size. To improve the FTBR, ground extension is made. The size reduction of the proposed design is implemented with half mode SIW topology. The gain and efficiency improved new DLSIW antenna is fabricated using FR4 material and it resonates at 5.27GHz WLAN frequency. The size of antenna is 44 mm × 18.75 mm × 1.6 mm and it has the gain of 5.824 dB. The radiation efficiency and FTBR of the antenna are 69.13% and 13.65 dB, respectively. The design is experimentally tested and compared with earlier WLAN antennas. There is a better accordance between simulated and measured results.

**KEYWORDS**

double line SIW, gain, half mode, radiation efficiency, WLAN

## 1 | INTRODUCTION

With the progress in wireless technology, there is a great demand for compact antennas with good efficiency and gain suitable for WLAN applications. The antennas that are designed for WLAN applications so far either lags in gain and radiation efficiency or in miniaturization. In Reference 1, a WLAN antenna fabricated with FR4 substrate achieves horizontal polarization with omnidirectional radiation pattern. But the size of the antenna is 120 mm × 54 mm. A multiband antenna applicable to GPS/WiMAX/WLAN with rectangular slot has been reported in Reference 2. This antenna achieves 4.482 dB gain at 5.2GHz and it has the size of 44 mm × 35 mm ×35 mm. In Reference 3, a wearable antenna for WLAN application using textile material has been reported. The antenna is designed with two "U" shaped slots for wide band character. But the efficiency of the antenna is around 50% and the antenna has gain of 4.7 dB. Also the antenna has large size and the fabrication cost of textile material is high. In Reference 4, a dual band antenna made with two layers of FR4 substrate suitable for WLAN and RFID applications has been reported. The antenna is circularly polarized and it achieves efficiency of 34% with gain of 1.8 dB at 2.4GHz. To get robust performance for transferring images from medical equipment through WLAN, an antenna that is embedded within metallic enclosures has been reported in Reference 5. This antenna has the gain of 1 dB and 2.3 dB at 2.4 GHz and 5 GHz, respectively. With the use of stacking technique, a dual band antenna[6] suitable for WLAN applications has been reported. The front to back ratio (FTBR) attained in the antenna is 10 dB. In Reference 7, SIW based textile antenna operating in dual bands for WLAN applications has been reported. The compactness is not attained as the antenna has the size of 92.3 mm × 101.9 mm × 3 mm and it is fabricated using textile substrate material. A monopole antenna with omnidirectional radiation pattern based on single line SIW (SLSIW) technology suited for WLAN applications is

  

presented in Reference 8 and it achieves a less gain of 2.38 dB. A SIW based triplexer applicable for radio altimeter, WLAN and ISM band is designed with radiating slots which is responsible for resonance at the three bands.[9] The antenna has unidirectional radiation pattern and it has the dimension of 85.71 mm × 64.28 mm with gain of 4.2 dB at 5.2GHz. A compact sized radiator with L shaped slots etched on the patch for operation in WLAN and WiMAX bands[10] has less gain of 3.74 dB at the WLAN frequency. A microstrip antenna with trapezoidal slot for dual band operation at WLAN and WiMAX applications[11] has the size of 35 mm × 30 mm × 1.6 mm. The gain achieved in the antenna is 4.32 dB at the WLAN band.

The conventional SLSIW technology has several advantages in terms of high gain, high antenna efficiency, high quality factor, and good power handling capabilities. Although it has several advantages, the existing SIW based antennas for WLAN applications are not compact. By using half mode SIW technique miniaturization is attained in antennas.[12-15]

From the above literature, it is observed that the simultaneous achievement of size reduction, better gain, and improved FTBR with good radiation efficiency is the research issue. This article proposes a compact double line substrate integrated waveguide (DLSIW) cavity backed antenna using half mode SIW technology for WLAN applications. Due to fact that the current distribution in proposed DLSIW structure is higher than SLSIW structure, the proposed design attains simultaneous improvement in the performance parameters (ie, gain, efficiency, and FTBR) with size reduction. The proposed antenna resonates at 5.27GHz with reflection coefficient ($S_{11}$) of −28.9 dB.

## 2 | ANTENNA DESIGN

The SLSIW technology is well suited for mitigating the radiation loss by removing the contribution of the dielectric material through metallic vias connecting the top and bottom plates of the metallic cavity. In DLSIW design, two lines of conducting SIW metallic vias are arranged along the side walls of the SIW cavity. As, the number of metallic vias increases, the removal of the dielectric material also increases in double line structure than the SLSIW structure. The DLSIW structure is designed by placing another line of SIW vias adjacent to the existing SIW vias placed along the side walls. Figures 1 and 2 show the side view and top view of SLSIW and DLSIW. The diameter of the vias is chosen as 1 mm and the spacing between vias is chosen as 1.6 mm satisfying the constraints $d/p \geq 0.5$ and $d/\lambda \leq 0.1$, where "$d$" denotes the diameter of vias and "$p$" denotes the spacing between vias. The SIW cavity is designed to resonate at frequency given by Equation (1).[14]

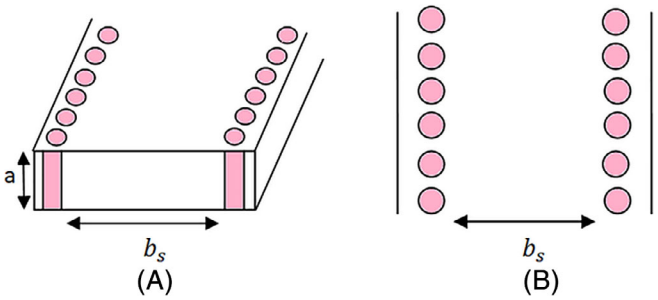


**FIGURE 1** Single line SIW. A, Side view. B, Top view. SIW, substrate integrated waveguide

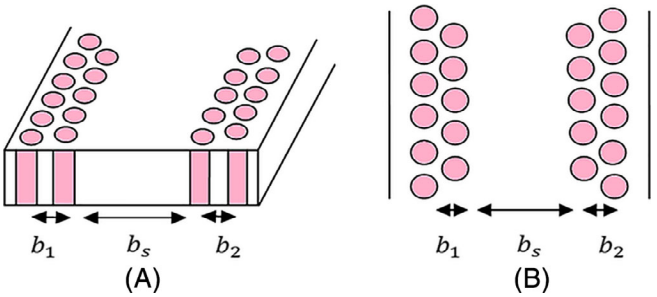


**FIGURE 2** Double line SIW. A, Side view. B, Top view. SIW, substrate integrated waveguide

$$f_{mn0} = \frac{c}{2\sqrt{\mu_{r}\epsilon_{r}}}\sqrt{\left(\frac{m}{L_{eff}}\right)^2 + \left(\frac{n}{W_{eff}}\right)^2} \quad (1)$$

where, $w_{eff}$ and $L_{eff}$ denotes the effective length and width of SIW cavity given in Equations (2) and (3).

$$w_{eff} = w_{HM} - \frac{d^2}{0.95p} \quad (2)$$

$$L_{eff} = L_{HM} - \frac{d^2}{0.95p} \quad (3)$$

The surface current distribution for the SLSIW structure in $TE_{01}$ and $TE_{11}$ modes are given in the Equations (4) and (5).

$$\overline{J_s TE_{01}} = \bar{x} \times \bar{z} A_{01} \cos\left(\frac{\pi y}{b_s}\right) e^{-j\beta z} + \bar{x} \times \bar{y} |H_y|_{x=0} \quad (4)$$

$$\overline{J_s TE_{11}} = \bar{x} \times \bar{z} A_{11} \cos\left(\frac{\pi y}{b_s}\right) e^{-j\beta z} + \bar{x} \times \bar{y} |H_y|_{x=0} \quad (5)$$

The Equations (4) and (5) can be modified by adding additional current components for the DLSIW structure and they are given in Equations (12) and (13). The width of SIW based on number of vias is given in Equation (6).

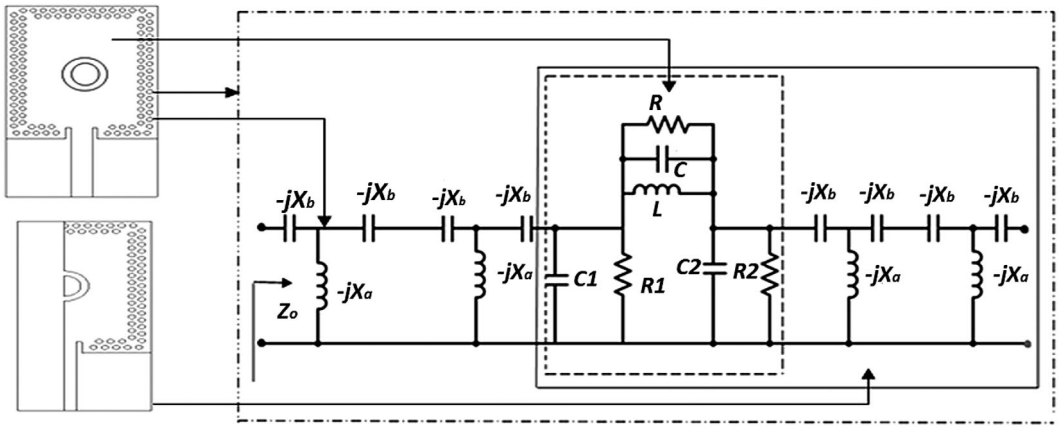


**FIGURE 3** Equivalent circuit model for double line SIW. SIW, substrate integrated waveguide

$$w_{\mathrm{SIW}} = nd + (n-1)(p-2r) \tag{6}$$

Here, "$n$" denotes the number of via holes and "$r$" denotes the radius of via holes. The vertical current path is not perturbed by the DLSIW arrangement. This leads to improvement in gain and radiation efficiency of the antenna which in turn increases the field strength and decreases the radiation loss. This can also be accomplished by placing SIW vias very close to each other with large diameter. Owing to decrease in dielectric loss with dielectric removal through SIW vias, the total radiated power increases. For double line structure, the surface current distribution on side walls of cavity with $\mathrm{TE}_{10}$ mode is given in Equation (7). The magnetic field strength along $z$ direction is given in Equation (8). The surface current distribution on the horizontal side walls of the DLSIW structure with $\mathrm{TE}_{10}$ mode is given by Equation (9).The terms $b_1$, $b_2$, $b_s$ denotes the width of the adjacent horizontal side walls of the SIW cavity.

$$\overline{J_s \mathrm{TE}_{10}} = \bar{x} \times \bar{z} H_z \tag{7}$$

$$H_z = A_{10} \cos\left(\frac{\pi x}{a}\right) \cos\left(\frac{2\pi z}{\lambda_g}\right) \tag{8}$$

$$\overline{J_s \mathrm{TE}_{10}} = -\bar{y}\left\{A_{10} \cos\left(\frac{\pi x}{a}\right) \cos\left(\frac{2\pi z}{\lambda_g}\right)\right\} \tag{9}$$

The surface current distribution for $\mathrm{TE}_{01}$ mode is given in Equation (10). This is simplified and given in Equation (11).

$$\begin{aligned}\overline{J_s \mathrm{TE}_{01}} = {} & \bar{x} \times \bar{z} A_{01} \cos\left(\frac{\pi y}{b_s}\right) e^{-j\beta z} + \bar{x} \times \bar{y} \left|H_y\right|_{x=0} \\ & + \bar{x} \times \bar{z} A_{01} \cos\left(\frac{\pi y}{b_1}\right) e^{-j\beta z} + \bar{x} \times \bar{y} \left|H_y\right|_{x=0} \\ & + \bar{x} \times \bar{z} A_{01} \cos\left(\frac{\pi y}{b_2}\right) e^{-j\beta z} + \bar{x} \times \bar{y} \left|H_y\right|_{x=0}\end{aligned} \tag{10}$$

$$\begin{aligned}\overline{J_s \mathrm{TE}_{01}} = {} & -\bar{y} A_{01} e^{-j\beta z}\left\{\cos\left(\frac{\pi y}{b_s}\right) + \cos\left(\frac{\pi y}{b_1}\right) + \cos\left(\frac{\pi y}{b_2}\right)\right\} \\ & + 3\bar{z}\left|H_y\right|_{x=0}\end{aligned} \tag{11}$$

Similarly, the surface current distribution for $\mathrm{TE}_{11}$ is given in Equation (12)

$$\begin{aligned}\overline{J_s \mathrm{TE}_{11}} = {} & \bar{x} \times \bar{z} A_{11} \cos\left(\frac{\pi y}{b_s}\right) e^{-j\beta z} + \bar{x} \times \bar{y} \left|H_y\right|_{x=0} \\ & + \bar{x} \times \bar{z} A_{11} \cos\left(\frac{\pi y}{b_1}\right) e^{-j\beta z} + \bar{x} \times \bar{y} \left|H_y\right|_{x=0} + \bar{x} \times \bar{z} A_{11} \\ & \cos\left(\frac{\pi y}{b_2}\right) e^{-j\beta z} + \bar{x} \times \bar{y} \left|H_y\right|_{x=0}\end{aligned} \tag{12}$$

This can be simplified and given in the Equation (13).

$$\begin{aligned}\overline{J_s \mathrm{TE}_{11}} = {} & -\bar{y} A_{11} e^{-j\beta z}\left\{\cos\left(\frac{\pi y}{b_S}\right) + \cos\left(\frac{\pi y}{b_1}\right) + \cos\left(\frac{\pi y}{b_2}\right)\right\} \\ & + 3\bar{z}\left|H_y\right|_{x=0}\end{aligned} \tag{13}$$

From Equations (11) and (13), it can be seen that the current distribution of the DLSIW is more as the current propagation is intense between two adjacent lines of SIW vias on either sides of the SIW cavity. This leads to increase in the field strength and it is responsible for increase in efficiency of the antenna. The higher current distribution tends to suppress the effect of surface waves and hence the leakage loss is reduced. Figure 3 shows the equivalent circuit model of proposed DLSIW structure.

The DLSIW design is modeled with RLC components in the equivalent circuit. As the SIW vias are embedded in dielectric medium, it is realized with two capacitors connected in series with inductor in shunt connection. Table 1 provides the

dimensions of the proposed antenna which are designed based on the Equations (1)-(3). Figures 4 and 5 describes the design of complete SLSIW and DLSIW structures, respectively.

The semicircular ring slot etched on the patch is to shift the resonant frequency from 4.9 to 5.2 GHz. The introduction of slots produces fringing effects. To achieve high FTBR, the ground extension is made. The metallic vias connecting the upper and lower plates of substrate is useful in preventing the leakage of energy from the side walls of SIW cavity. The substrate is designed with the thickness of 1.6 mm. When the antenna is bisected along $A - A'$, the full mode structure becomes half mode and hence the ground occupancy in the antenna is reduced. There is a gain reduction due to the contribution of large back lobes in small sized ground plane. The small sized ground plane leads to the formation of surface waves as there is a decrease in field strength normal to the direction of antenna. These surface waves propagate at the edges of the ground plane. The efficiency of the surface waves depends on substrate thickness, dielectric constant, and current distribution of the antenna. When the current distribution increases, the contribution of the surface waves is reduced. Thus front to back reflections are minimized which increases the FTBR greater than 13 dB.

**TABLE 1** Dimensions of proposed antenna

| Parameters | Dimension (mm) |
|---|---|
| $L$ | 44 |
| $W$ | 24.5 |
| $w_{HM}$ | 12.25 |
| $L_{HM}$ | 30.6 |
| $w_f$ | 1.7 |
| $Gnd_{ext}$ | 6.5 |
| $w_{slot}$ | 1.1 |
| $p$ | 1 |
| $d$ | 1.6 |

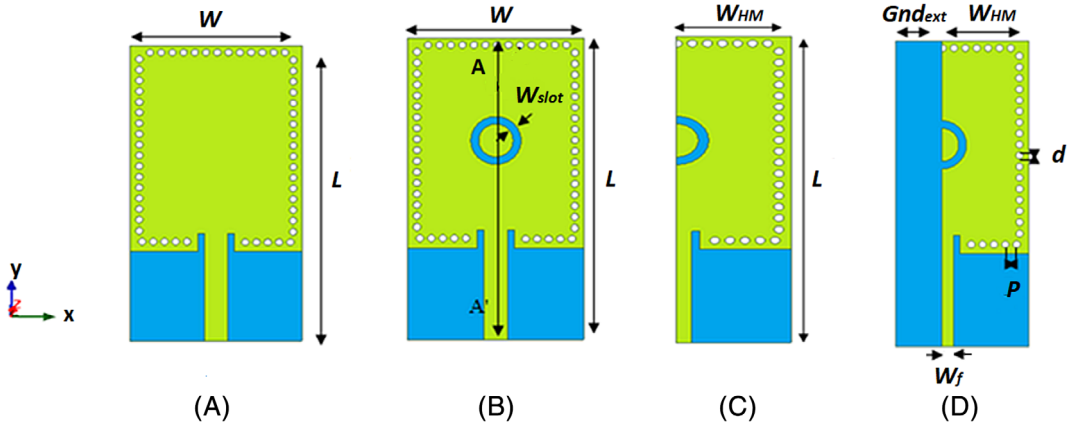


**FIGURE 4** Single line SIW structures. A, Full mode. B, Full mode with circular ring slot. C, Half mode SIW with semicircular ring slot. D, Ground extended design. SIW, substrate integrated waveguide

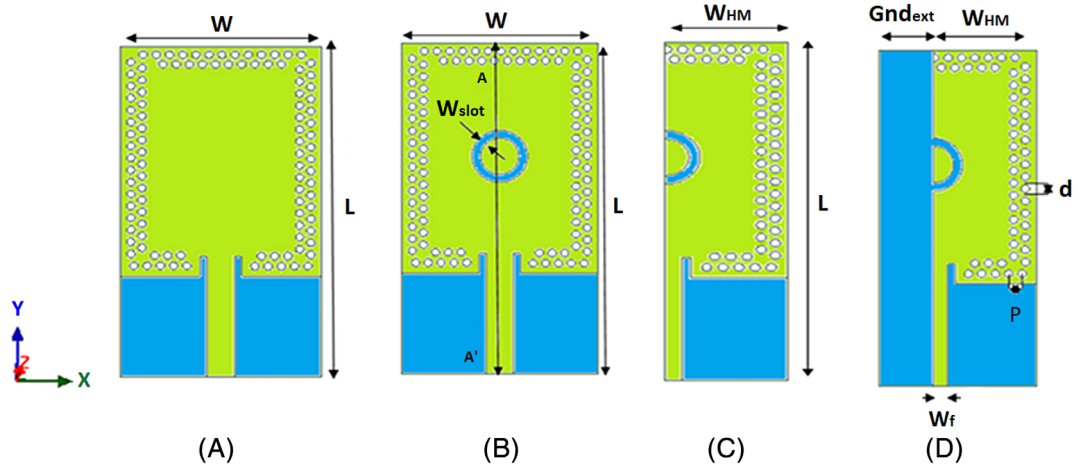


**FIGURE 5** Double line SIW structures. A, Full mode. B, Full mode with circular ring slot. C, Half mode SIW with semicircular ring slot. D, Proposed DLSIW. DLSIW, double line substrate integrated waveguide; SIW, substrate integrated waveguide

**TABLE 2** Performance comparison of single line and double line SIW topologies—simulated

| Antenna structure | Gain (dB) | Directivity (dB) | Radiation efficiency (%) | Frequency (GHz) | Reflection coefficient (dB) |
|---|---|---|---|---|---|
| Single line full mode | 1.07 | 4.05 | 50.30 | 4.8 | −18.00 |
| Double line full mode (DLFM) | 2.45 | 5.46 | 50.50 | 4.9 | −33.20 |
| Single line full mode with slot | 3.48 | 6.12 | 53.70 | 4.7 | −13.20 |
| Double line full mode with slot | 3.975 | 6.49 | 55.90 | 5.0 | −17.70 |
| Single line half mode | 3.26 | 5.36 | 61.60 | 5.1 | −16.30 |
| Double line half mode (DLHM) | 3.97 | 5.43 | 62.50 | 5.2 | −20.90 |
| Single Line (GroundExtended) | 5.091 | 7.616 | 66.70 | 5.166 | −29.17 |
| DLSIW | 5.824 | 7.428 | 69.13 | 5.26 | −20.24 |

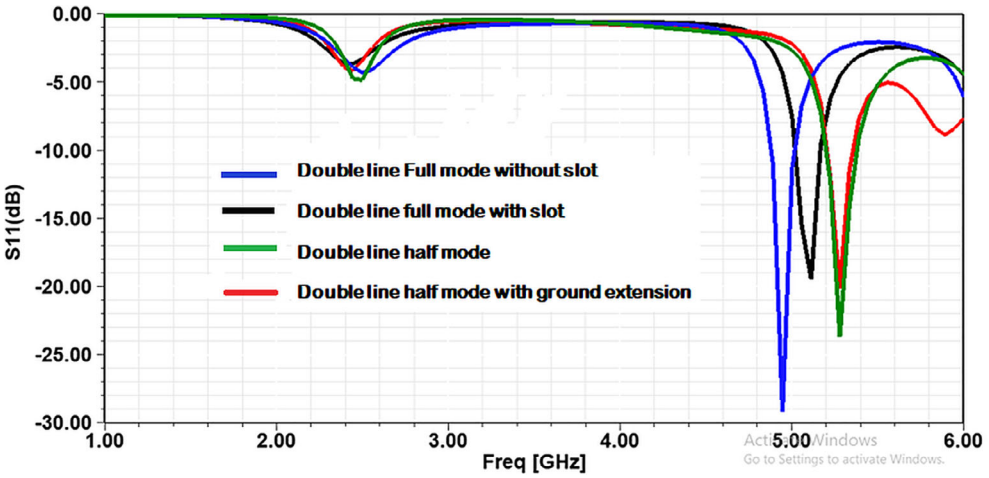


**FIGURE 6** Simulated frequency versus reflection coefficient plot for DLFM, DLFM with circular ring slot, DLHM with semicircular ring slot and DLSIW. DLFM, double line full mode; DLHM, double line half mode; DLSIW, double line substrate integrated waveguide

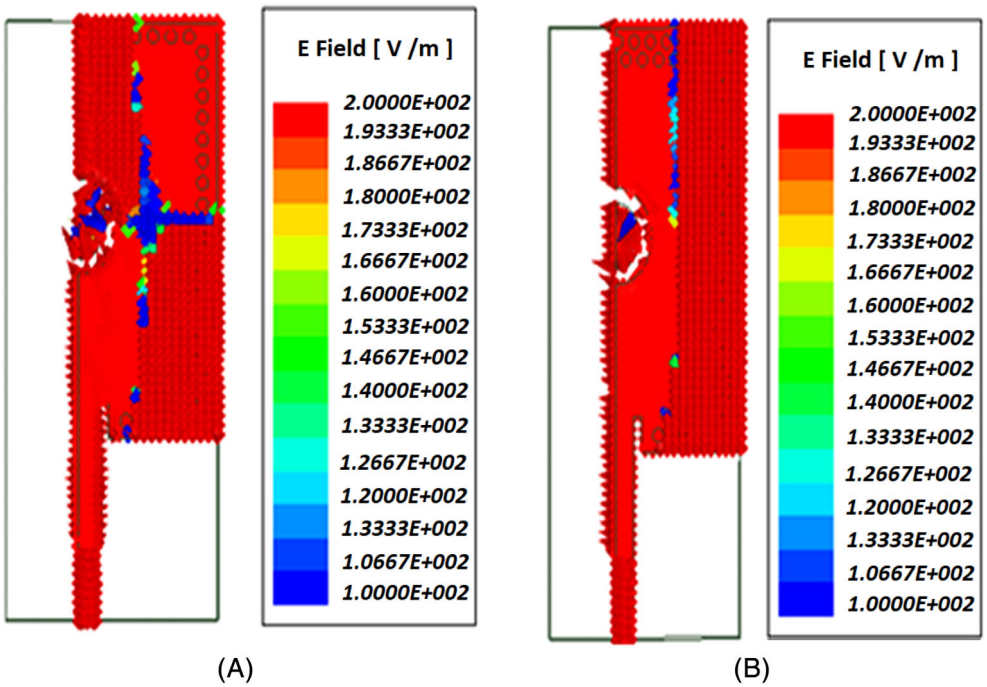


**FIGURE 7** Current distribution of ground extended design. A, SLSIW at 5.16GHz. B, DLSIW at 5.26 GHz. DLSIW, double line substrate integrated waveguide; SLSIW, single line SIW

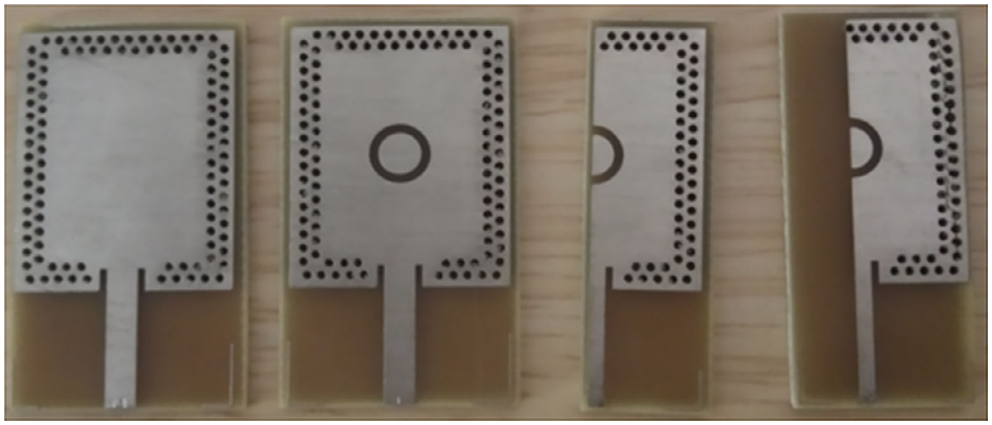

**FIGURE 8** Fabricated prototypes of double line SIW topologies. SIW, substrate integrated waveguide

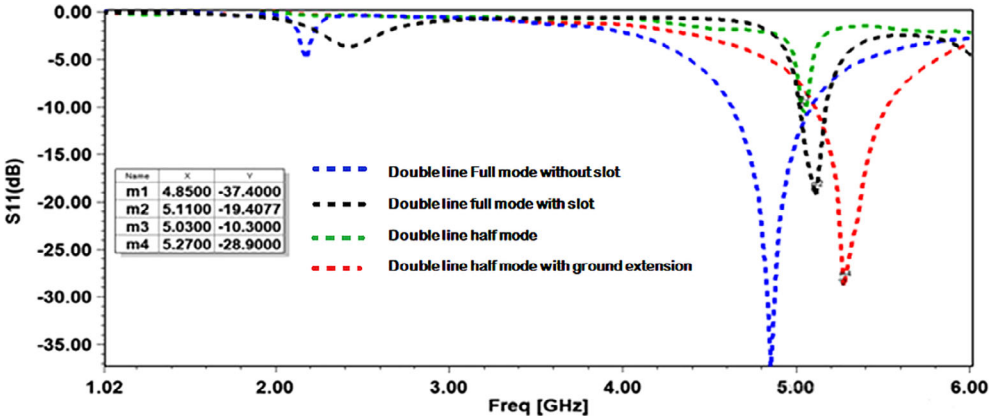


**FIGURE 9** Measured frequency versus reflection coefficient plot for DLFM, DLFM with circular ring slot, DLHM with semicircular ring slot and DLSIW. DLFM, double line full mode; DLHM, double line half mode; DLSIW, double line substrate integrated waveguide

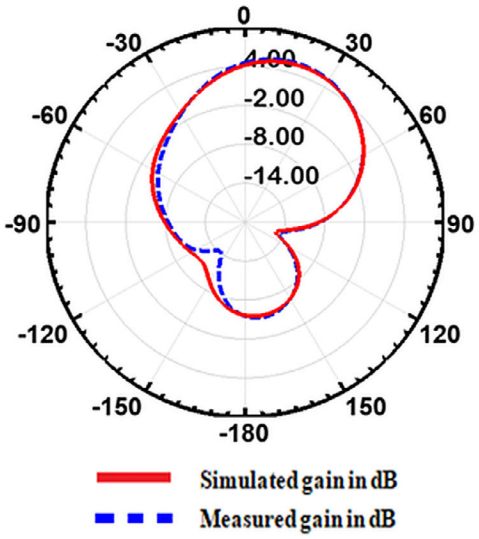


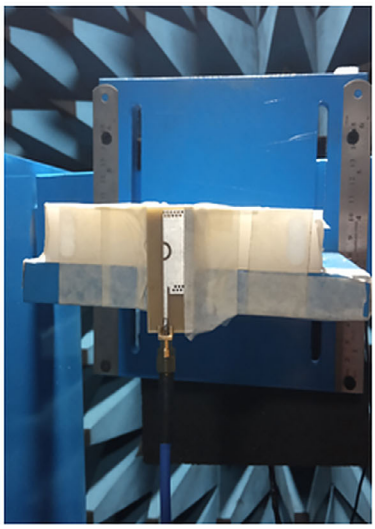

**FIGURE 10** Simulated and measured gain plot at 5.26 GHz

## 3 | RESULTS AND DISCUSSIONS

To prove the ability of DLSIW, the SLSIW and DLSIW structures in (a) full mode, (b) full mode with circular ring slot, (c) half mode SIW with semicircular ring slot, and (d) ground extended design are simulated and the performance of antenna parameters are compared in Table 2. From Table 2, it can be inferred that the performance of the DLSIW structure in terms of gain and efficiency is better than SLSIW structure. The simulated frequency versus reflection coefficient plot for all double line SIW topologies (ie) double line full mode (DLFM), DLFM with circular ring slot, double line half mode (DLHM), DLHM with semicircular ring slot and DLSIW are shown in Figure 6.

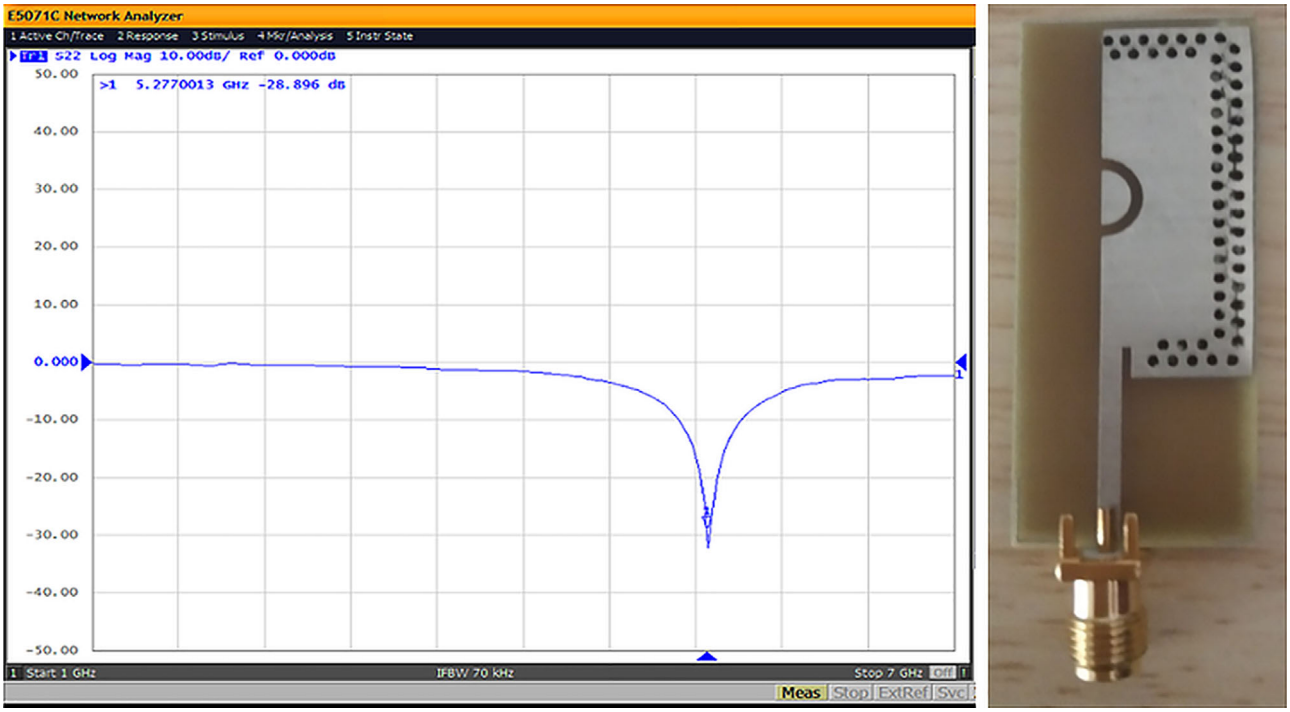


**FIGURE 11** Measured frequency versus reflection coefficient plot for DLSIW using Vector Network Analyzer. DLSIW, double line substrate integrated waveguide

**TABLE 3** Performance comparison of proposed antennas with previous antennas

| References | Dimension | Materials | Frequency (GHz) | Applications | Gain (dB) | Efficiency (%) | FTBR (dB) |
|---|---|---|---|---|---|---|---|
| 2 | 44 × 35 $mm^2$ | RO4003C | 1.5/2.4/3.5/5.2 | GPS/WiMAX/WLAN | 1.3/2.3 3.5/4.48 | 76.8/80.1/96.6/85.5 | NA |
| 3 | 100 × 100 $mm^2$ | Textile | 2.4/5.8 | WLAN/WBAN | 4.7/3 | >50/>60 | >10 |
| 4 | 60 × 60 × 7 $mm^3$ | FR4 | 0.92/2.48 | RFID/WLAN | −0.1/1.8 | 50/34 | NA |
| 5 | 64 × 54 × 7 $mm^3$ | RO4003C | 2.45/ 5 | WLAN | 1/2.3 | NA | NA |
| 7 | 92.3 × 101.9 × 3 $mm^3$ | Textile | 2.4/ 5 | WLAN | 3.2/2.9 | >55/60 | NA |
| 9 | 85.71 × 64.28 $mm^2$ | RT 5880 | 4.18/5.2/5.8 | Radio altimeter/WLAN/ISM | 6.5/4.2/5.85 | NA | >19 |
| 12 | 2080 $mm^2$ | Textile | 2.4/ 5.8 | WLAN/WBAN | 4.4/5.7 | 72.8/85.6 | NA |
| 13 | 32.7 × 44 $mm^2$ | RT 5880 | 5/5.8 | WLAN/WBAN | 6.25/ 6 | 81.5 | >15 |
| 14 | 44 × 18.75 × 1.6 $mm^3$ | RO4003C | 5.8 | WBAN | 6.1 | 83 | >10 |
| 15 | 19 × 19 $mm^2$ | RT 5880 | 5.5/5.8 | WLAN/WBAN | 4.5/4.8 | 89.4 | NA |
| DLSIW in full mode | 44 × 24.5 × 1.6 $mm^3$ | RO4003C | 5.44 | WLAN | 6.64 | 89.96 | >9 |
| Proposed DLSIW | 44 × 18.75 × 1.6 $mm^3$ | RO4003C | 5.8 | WLAN[16] | 6.657 | 92.8 | >9 |
| | 44 × 18.75 × 1.6 $mm^3$ | FR4 | 5.26 | WLAN | 5.824 | 69.13 | >13 |

Abbreviations: DLSIW, double line substrate integrated waveguide; FTBR, front to back ratio.

The current distribution between two lines of SIW cavity is more intense than the SLSIW cavity. The current distribution is proportional to the efficiency of antenna. The DLSIW structure has higher current distribution than SLSIW structure. Hence the efficiency of DLSIW arrangement is better than SLSIW arrangement. The vector current distribution of ground extended SLSIW at 5.16 GHz and ground extended DLSIW design at 5.26GHz are shown in Figure 7. All the double line SIW topologies resonate at WLAN frequency with good $S_{11}$ as shown in Table 2. To validate the proposed design, all the double line topologies are fabricated with FR4 substrate. The fabricated double line topologies that are shown in Figure 8 are

experimentally tested and they have the VSWR < 2. The measured frequency versus reflection coefficient plot for all DLSIW structures are shown in Figure 9. The measured and simulated results are in good agreement. The gain plot for DLSIW has been depicted in Figure 10. The proposed antenna while validating has the measured gain of 5.5 dB at 5.26 GHz. The energy of the antenna is distributed over less area and hence the signal strength increases which is responsible for increasing the directivity of antenna. The DLSIW structure exhibits bidirectional radiation pattern. Figure 11 shows the measured frequency versus reflection coefficient plot for DLSIW topology using vector network analyzer.

The performance comparison of proposed antenna with previous antennas is shown in Table 3. Antennas, only operating in the WLAN frequency are considered for comparison. In Table 3, the mentioned antenna materials are as given in their original work. From Table 3, it is inferred that the proposed DLSIW structure has better gain, efficiency, and FTBR even with FR4 substrate. The DLSIW (full mode), proposed DLSIW shown in Figure 5A,D when simulated with RO4003C has gain of 6.64 dB and 6.657 dB, respectively, which are better when compared to the previous antennas that were realized using the same lossless substrate (RO4003C).

## 4 | CONCLUSION

This research article presents a novel design of DLSIW cavity backed antenna for WLAN applications. This compact DLSIW cavity backed antenna is realized to overcome the limitations of existing low gain and less efficiency SLSIW antennas for WLAN applications. The new DLSIW structure simultaneously achieves better gain, radiation efficiency, and good FTBR with compact size. This two line arrangement of SIW vias along the side walls of cavity exhibits a good agreement with measured and simulated counterparts. The proposed design has the advantages of compact size, VSWR of 1.28, good radiation performance, and acceptable gain with low cost FR4 substrate.

## ORCID

*Swaminathan Anand* https://orcid.org/0000-0002-0307-1942

## REFERENCES

1. Lin CC, Kuo LC, Chuang HR. A horizontally polarized omnidirectional printed antenna for WLAN applications. *IEEE Trans Antennas Propag*. 2006;54(11):3551-3556.
2. Cao YF, Cheung SW, Yuk TI. A multiband slot antenna for GPS/WiMAX/WLAN systems. *IEEE Trans Antennas Propag*. 2015;63(3):952-958.
3. Yan S, Soh PJ, Vandenbosch GA. Wearable dual-band magneto-electric dipole antenna for WBAN/WLAN applications. *IEEE Trans Antennas Propag*. 2015;63(9):4165-4169.
4. Caso R, Michel A, Rodriguez-Pino M, Nepa P. Dual-band UHF-RFID/WLAN circularly polarized antenna for portable RFID readers. *IEEE Trans Antennas Propag*. 2014;62(5):2822-2826.
5. Soh PJ, Yan S, Xu H, Vandenbosch GA. A dual-band cavity antenna embedded within multiple metallic enclosures. *IEEE Trans Antennas Propag*. 2016;64(5):1587-1594.
6. Pushpakaran SV, Raj RK, Vinesh PV, Dinesh R, Mohanan P, Vasudevan K. A metaresonatorinspired dual band antenna for wireless applications. *IEEE Trans. Antennas Propag*. 2014;62(4):2287-2291.
7. Yan S, Soh PJ, Vandenbosch GA. Dual-band textile MIMO antenna based on substrate-integrated waveguide (SIW) technology. *IEEE Trans Antennas Propag*. 2015;63(11):4640-4647.
8. Hanumanthappa RI. SIW based mono-pole antenna for WLAN and WIMAX applications. 2017 2nd IEEE International Conference on Recent Trends in Electronics, Information & Communication Technology (RTEICT), Bangalore; May 19, 2017; IEEE: 1010-1013.
9. Chaturvedi D, Kumar A, Raghavan S. An integrated SIW cavity-backed slot antenna-triplexer. *IEEE Antennas Wirel Propag Lett*. 2018;17(8):1557-1560.
10. Chen H, Yang X, Yin YZ, Fan ST, Wu JJ. Triband planar monopole antenna with compact radiator for WLAN/WiMAX applications. *IEEE Antennas Wirel Propag Lett*. 2013;12:1440-1443.
11. Dang L, Lei ZY, Xie YJ, Ning GL, Fan J. A compact microstrip slot triple-band antenna for WLAN/WiMAX applications. *IEEE Antennas Wirel Propag Lett*. 2010;9:1178-1181.
12. Agneessens S, Rogier H. Compact half diamond dual-band textile HMSIW on-body antenna. *IEEE Trans Antennas Propag*. 2014;62(5):2374-2381.
13. Chaturvedi D, Raghavan S. A dual-band half-mode substrate integrated waveguide-based antenna for WLAN/WBAN applications. *Int J RF Microw Comput Aided Eng*. 2018;28(5):e21239.
14. Chaturvedi D, Raghavan S. A half-mode SIW cavity-backed semi-hexagonal slot antenna for WBAN application. *IETE J Res*. 2018;1-7.
15. Chaturvedi D, Raghavan S. Compact QMSIW based antennas for WLAN/WBAN applications. *Prog Electromagn Res*. 2018;82:145-153.
16. Han W, Yang F, Long R, Zhou L, Yan F. Single-fed low-profile high-gain circularly polarized slotted cavity antenna using a high-order mode. *IEEE Antennas Wirel Propag Lett*. 2016;15:110-113.

## AUTHOR BIOGRAPHIES

**Swaminathan Anand** received his BE Degree in Electronics and Communication Engineering, 1991, ME degree in Communication Systems, 2002 and PhD degree from Anna University Chennai. He is a life time member of ISTE, IETE, and ISCA. His current research interests include Antenna Design and Image Processing. He had 25 years of teaching and research experience. Currently he is working as Professor, Electronics and Communication Engineering, Mepco Schlenk Engineering College, Sivakasi, Tamil Nadu, India. He

has published more than 100 research articles in reputed journals and conferences.

**D. Rokhini** was born in India. She received her BE Degree in Electronics and Communication Engineering, 2017 and ME degree in Communication Systems, 2019 from Mepco Schlenk Engineering College, affiliated to Anna University Chennai. Her research interests include SIW Antenna modes and metasurfaces.

**How to cite this article:** Anand S, Rokhini D. A double line SIW cavity backed antenna for WLAN applications. *Int J RF Microw Comput Aided Eng*. 2019;e21861. https://doi.org/10.1002/mmce.21861